

Sunspot Structure*

Sanjiv K. TIWARI^{1,2,3,4#}

¹NASA Marshall Space Flight Center, Mail Code ST 13, Huntsville, AL 35812, USA

²Center for Space Plasma and Aeronomic Research, University of Alabama in Huntsville, AL 35899, USA

³Lockheed Martin Solar and Astrophysics Laboratory, 3251 Hanover Street, Building 252, Palo Alto, CA 94304, USA

⁴Bay Area Environmental Research Institute, NASA Research Park, Moffett Field, CA 94035, USA

*E-mail: tiwari@lmsal.com

Received ; Accepted

Abstract

Sunspots contain multiple small-scale structures in the umbra and in the penumbra. Despite extensive research on this subject in pre-Hinode era multiple questions concerning fine-scale structures of sunspots, their formation, evolution and decay remained open. Several of those questions were proposed to be pursued by Hinode (SOT). Here we review some of the achievements on understanding sunspot structure by Hinode in its first 10 years of successful operation. After giving a brief summary and updates on the most recent understanding of sunspot structures, and describing contributions of Hinode to that, we also discuss future directions. This is a section (#7.1) of a long review article on the achievements of Hinode in the first 10 years.

Key words: Sun: photosphere — Sun: magnetic fields — sunspots

1 Introduction

Sunspots, dark features on the surface of the Sun due to the suppressed convection owing to the presence of strong magnetic field in them, contain multiple small-scale structures in the central darkest part, the umbra, and in the less-dark region surrounding the umbra, the penumbra (figure 1). The magnetic, thermal, and flow structures of sunspots were extensively studied in the pre-Hinode era. But multiple questions pertaining to sunspot fine structure, their formation, evolution and decay, remained open, requiring a closer look. Some of these questions were proposed to be pursued by Hinode (SOT). For example, what are the internal structures of basic umbral and penumbral features (i.e., umbral dots, umbral dark area, light bridges, penumbral filaments, spines, penumbral bright grains) of sunspots and how are these basic um-

bral and penumbral structures formed and maintained? What drives the Evershed flow in sunspot penumbra in the photosphere and the inverse Evershed flow in sunspot penumbra in the chromosphere? How do the basic sunspot structures disintegrate in magnetic fragments and diffuse to the quiet Sun? How do moving magnetic features form and what is their role in sunspot decay? Are umbral dots, light bridges, penumbral filaments (magneto)convection cells, as suggested by recent numerical modellings?

High spatial resolution, precise, and high signal-to-noise observations by the Solar Optical Telescope (Ichimoto et al. 2008b; Shimizu et al. 2008b; Suematsu et al. 2008; Tsuneta et al. 2008) on-board Hinode (Kosugi et al. 2007) have extraordinarily contributed to understanding of sunspot structure and dynamics, in the first 10 years, by providing new information about many sunspot features, including umbral dots, light bridges, penumbral filaments, moat regions, and disclosed their internal structures. Hinode helped addressing several of the

* Can be cited as: Tiwari, Sanjiv K. and Hinode Review Team, "Achievements of Hinode in the First Ten Years," 2018, PASJ, under review.
#Now with the affiliations 3 (LMSAL) and 4 (BAERI).

above-mentioned questions, and opened new directions. See Solanki (2003) for a detailed review on sunspot structure and for open questions thereon before the Hinode-era.

In this section (1), we review some of the latest developments, achieved from the data of unprecedented high quality obtained by Hinode, in establishing (mostly photospheric) thermal, flow and magnetic properties of sunspot structures both at small and global scales. Note that although works on umbral dots, light bridges, moving magnetic features, umbral/penumbral jets, and formation/decay of sunspots are reviewed, a more extensive detail is given on the fine-structure of the sunspot penumbra, the most complicated magnetic structure on the surface of the Sun, to understanding of which the Hinode has contributed the most significantly. We also discuss some questions that have emerged as a result of these new observations, i.e., about sunspot structure, dynamics and their connection with the upper atmosphere, and point out the need of multi-height/multi-temperature observations at a higher spatial resolution and cadence that are needed to answer them and that are anticipated from future generation solar telescopes e.g., DKIST and the next Japan-led solar space mission.

For past reviews on the structure of sunspots, please see Moore (1981), Spruit (1981), Moore & Rabin (1985), Schmidt (1991), Sobotka (1997), Solanki (2003), Thomas & Weiss (2004, 2008), Scharmer (2009), Tritschler (2009), Borrero & Ichimoto (2011), and Rempel & Schlichenmaier (2011). In recent years MHD simulations have made significant progress in reproducing many aspects of small-scale structures of sunspots (Hurlburt et al. 1996; Hurlburt & Rucklidge 2000; Schüssler & Vögler 2006; Heinemann et al. 2007; Scharmer et al. 2008; Rempel et al. 2009; Rempel & Schlichenmaier 2011; Rempel 2012). In this review, we mainly focus on the observational results and, when suitable, mention relevant simulations.

2 Umbral dots and light bridges

Sunspot umbrae often contain light bridges (LBs) and umbral dots (UDs); both are enhanced bright structures inside dark umbrae, magnetoconvection being a proposed mechanism of heat transport in them (Weiss 2002; Schüssler & Vögler 2006; Kitai et al. 2007; Watanabe et al. 2009; Watanabe 2014). Using Hinode/SOT-SP data, Riethmüller et al. (2008) detected upflows of 800 m s^{-1} , and a field weakening of some 500 G in UD; see also Sobotka & Jurčák (2009) and Feng et al. (2015) for a comparison of central and peripheral UD. Riethmüller et al. (2013) further analyzed the same sunspot data using a more sophisticated inversion technique and detected systematic diffuse downflows surrounding UD, consistent with the downflows seen by Ortiz et al. (2010) in a few UD of a pore. Riethmüller et al. (2013) further found that upflowing mass flux in central part of UD balances well with the downflowing mass flux in

their surroundings. Evidence of dark lanes in UD, as predicted by MHD simulations of Schüssler & Vögler (2006), was reported by Bharti et al. (2007) and Rimmele (2008). On the other hand, Louis et al. (2012) and Riethmüller et al. (2013) could not detect it, thus questioning the magnetoconvective nature of UD. Furthermore, MHD simulations suggest concentrated downflows at the UD boundary, not found in observations so far.

LBs, often apparent as a lane of UD, separate sunspot umbrae into two or more parts of the same polarity magnetic field. They can be divided into ‘granular’ photospheric substructures (e.g., Lites et al. 1991; Rouppe van der Voort et al. 2010; Lagg et al. 2014), ‘faint’ LBs (Lites et al. 1991; Sobotka & Puschmann 2009), or ‘strong’ LBs (Rimmele 2008; Rezaei et al. 2012). Similar to UD, magnetic fields in all types of LBs are more inclined from vertical as compared to their surroundings (Jurčák et al. 2006; Katsukawa et al. 2007a; Lagg et al. 2014; Felipe et al. 2016), and similar to the convergence of spine field over penumbral filaments (described later), umbral field converges above LBs. Supporting their convective nature, upflows in central part of LBs and surrounding strong downflows have been observed (Rimmele 1997; Hirzberger et al. 2002; Louis et al. 2009; Rouppe van der Voort et al. 2010; Lagg et al. 2014). Dark lanes have been detected in LBs using Hinode data by e.g., Bharti et al. (2007) and Lagg et al. (2014), thus supporting the magnetoconvective nature of LBs. Lagg et al. (2014) found field-free regions in granular LBs with similarities to “normal” quiet-Sun granules, thus suggesting that, unlike other umbral features (i.e., UD and other types of LBs), granular LBs could be made by convection from deeper layers. In a recent work by using Hinode SOT-SP time series of a sunspot, Okamoto & Sakurai (2018) found a LB to have the strongest magnetic field over the sunspot.

Several small-scale jet-like events in connection with UD and LBs have also been reported using Hinode data (e.g., Shimizu et al. 2009; Shimizu 2011; Louis et al. 2014; Bharti 2015; Toriumi et al. 2015; Yuan & Walsh 2016).

3 Structure of sunspot penumbral filaments

With the presence of rapidly varying fine-scale field, flow, and thermal properties, both in radial and azimuthal directions, sunspot penumbra represents, undoubtedly, the most complicated and challenging structure on the solar surface. Penumbrae are made of copious thin bright filaments (Title et al. 1993; Rimmele 1995; Langhans et al. 2005; Ichimoto et al. 2007b; Borrero & Ichimoto 2011) and dark spines (Lites et al. 1993). See also Su et al. (2009) and Tiwari et al. (2009b) for fine-scale distribution of local magnetic twists and current densities in sunspot penumbrae, and Tiwari et al. (2009a) and Gosain et al. (2010) for the effect of polarimetric noise in esti-

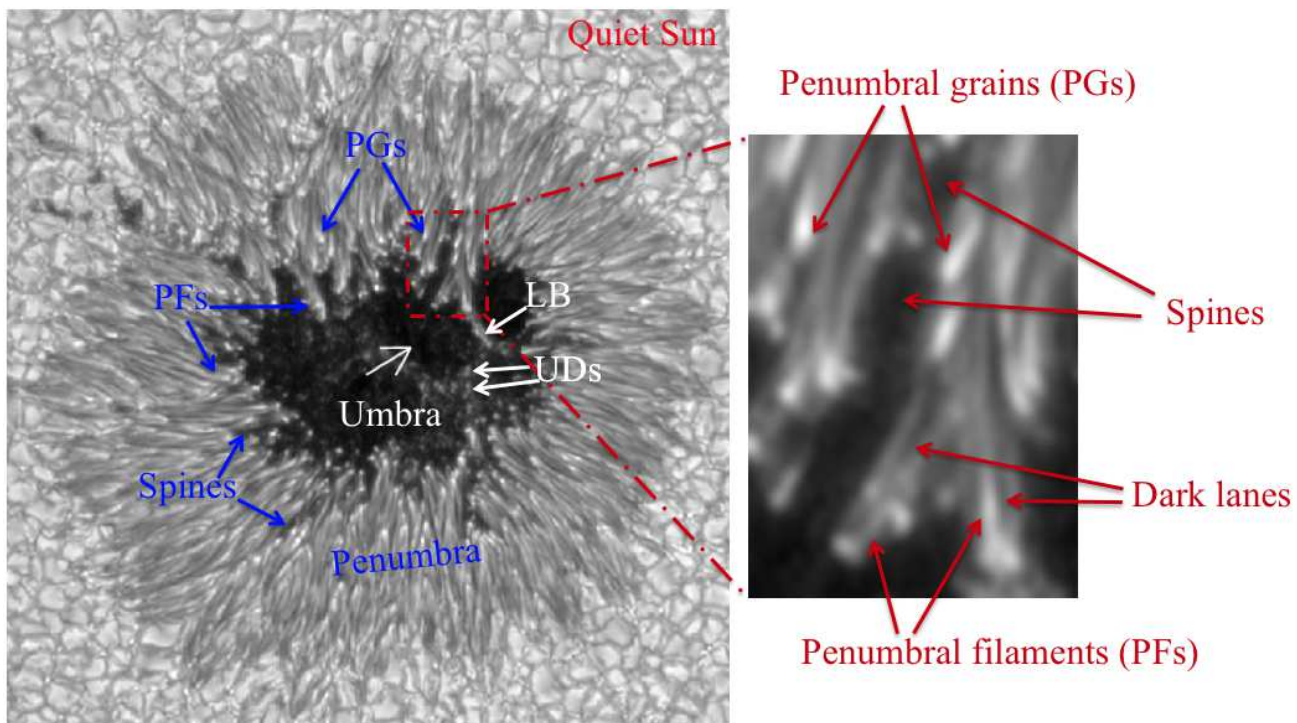


Fig. 1. Left: Continuum intensity image of a sunspot observed by Hinode/SOT-SP [reproduced from Tiwari et al. (2015) by permission of ESO]. Locations of a couple of umbral dots (UDs), penumbral filaments (PFs), spines, penumbral grains (which are actually heads of filaments) and a light bridge (LB), are pointed to by arrows. A larger arrow in the center of the sunspot umbra points to the direction of the solar disk center. The scale of the picture is $64'' \times 64''$. To clearly visualize the penumbral features (including dark lanes on penumbral filaments) a zoomed in view of a small FOV of the sunspot penumbra, outlined by dash-dotted box, is displayed in the right.

inating these parameters using Hinode data.

According to theoretical expectations (Cowling 1953; Schlüter & Temesváry 1958; Spruit 1977; Jahn & Schmidt 1994; Thomas & Weiss 2008; Priest 2014), the presence of strong magnetic field of 1–2 kG should prohibit convection in sunspot penumbrae, thus, keeping them dark, similar to umbrae. As penumbrae have some 75% brightness of quiet-Sun intensity, some form of convection takes place therein. It may be radial, i.e., upflows take place in the inner penumbrae and downflows in the outer penumbrae. Or there could be azimuthal/lateral convection, in that upflows take place all along the filament's central axis and downflows along the sides of the filament. Or the convection in penumbrae may be a combination of the above two (Borrero & Ichimoto 2011). The presence of radial convection was evidenced by e.g., Rimmele & Marino (2006), Ichimoto et al. (2007b), Tiwari et al. (2013), and Franz & Schlichenmaier (2009, 2013). Support for azimuthal convection was found by Ichimoto et al. (2007b), Zakharov et al. (2008), Bharti et al. (2010), Joshi et al. (2011), Scharmer et al. (2011), Scharmer & Henriques (2012), Tiwari et al. (2013), and Esteban Pozuelo et al. (2015), while other researchers could not detect such downflows (Franz & Schlichenmaier 2009; Bellot Rubio et al. 2010; Puschmann et al. 2010). Furthermore, convection in the penumbra can take place in the presence of strong

magnetic field (Rempel et al. 2009; Rempel & Schlichenmaier 2011; Rempel 2012), or in a very weak field or in absence of it (field-free gaps) [Scharmer & Spruit 2006; Spruit & Scharmer 2006].

By using Hinode/SOT-SP data of a sunspot (leading-polarity sunspot of NOAA AR 10933) observed almost on the solar disk center ($\mu = 0.99$) on 2007 January 5 (during 12:36–13:10 UT), Tiwari et al. (2013) explored the fine structure of penumbral filaments. Tiwari et al. (2015) then studied global properties of the same sunspot in light of the fine structure of filaments and spines, and sorted-out the thermal, velocity, and magnetic structures of the whole sunspot. In the following we summarize some of the main results found in these papers, with appropriate discussion and additional topics included. Interestingly, different aspects of Hinode data of this particular sunspot has been studied by several researchers, which has resulted in many other publications (e.g., Kubo et al. 2008b; Franz & Schlichenmaier 2009; Tiwari 2009, 2012; Tiwari et al. 2009b; Venkatakrishnan & Tiwari 2009, 2010; Katsukawa & Jurčák 2010; Borrero & Ichimoto 2011; Franz 2011; Riethmüller et al. 2013; van Noort et al. 2013; Joshi et al. 2017).

Inversion of Hinode (SOT/SP) data: Before we discuss new findings on small-scale structure of sunspots, we summarize

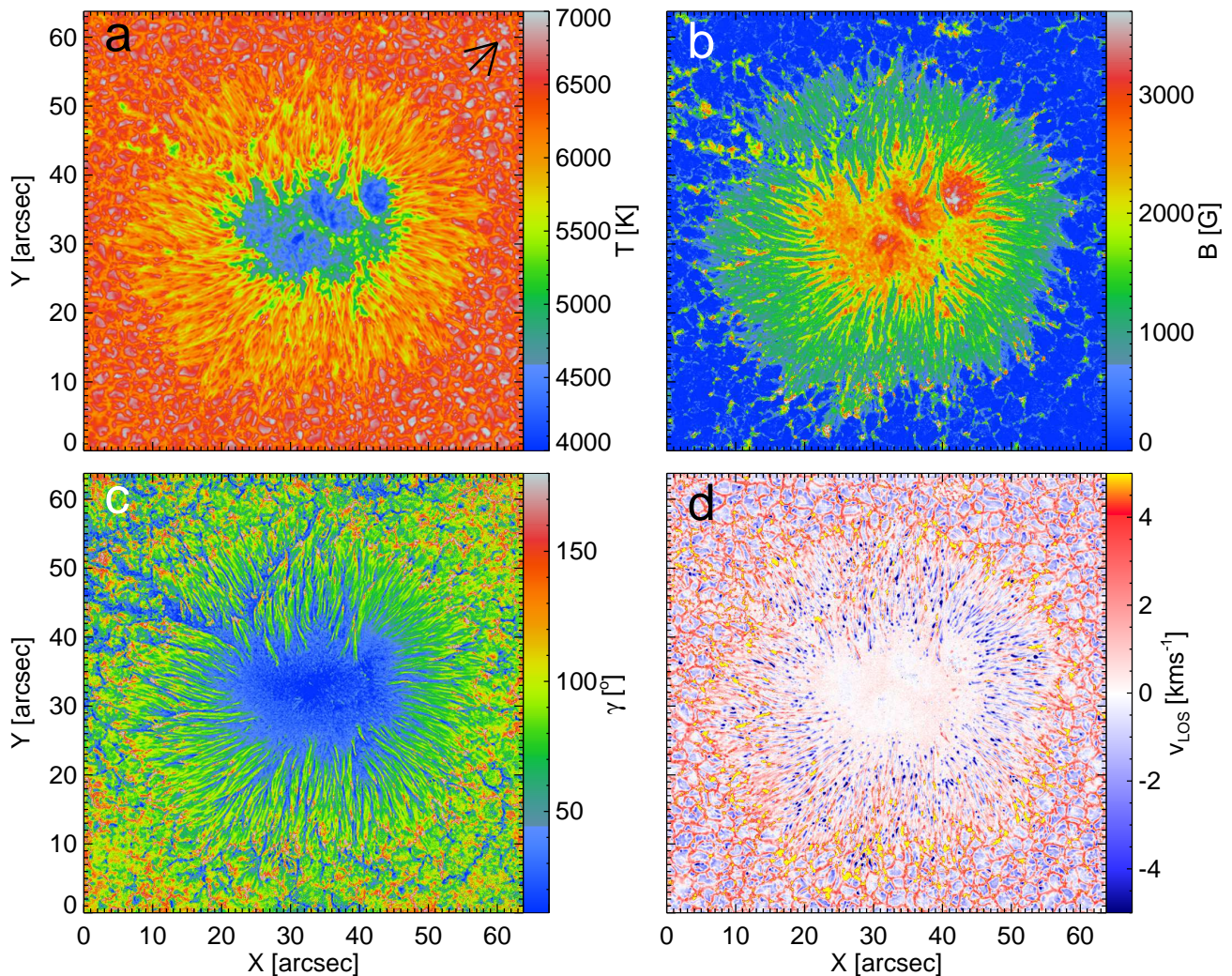


Fig. 2. Four selected maps of physical parameters of the leading positive magnetic polarity sunspot from AR 10933, observed by Hinode/SOT-SP and inverted using spatially coupled inversions. (a) T map; a black arrow points to the solar disk center. (b) B map. (c) γ map. (d) v_{LOS} map. Color bars for the parameters are attached to the right of each panel of the figure, and are scaled to enhance the visibility of spatial variations in the parameters. [Reproduced from Tiwari et al. (2015) by permission of ESO.]

here what sort of spectropolarimetric inversions were developed on Hinode SOT-SP data (due to known telescope parameters, e.g., Danilovic et al. 2008), and used to get many of the results described later. To infer physical parameters from the observed Stokes profiles different Milne-Eddington (the simplest model) and depth-dependent inversions (based on response functions) have been traditionally used (Skumanich & Lites 1987; Ruiz Cobo & del Toro Iniesta 1992; Socas-Navarro et al. 1998; Frutiger et al. 2000; Lagg et al. 2004; Asensio Ramos et al. 2008). Although we do not have to deal with the effects of the earth's atmosphere in the spectropolarimetric data of Hinode, we do have to deal with the spatial and spectral degradation caused by the telescope and the detector. In particular the spectral degradation was taken into account by Orozco Suárez et al. (2007) considering the local straylight as a second atmospheric component, which was considered to be contributed by telescope diffraction and not by unresolved small-scale struc-

ture. In this method of inversions, a significant amount of the signal ($\sim 75\%$ due to telescope diffraction) gets subtracted from each pixel, thus, significantly reducing the signal-to-noise ratio of the results. To properly take in to account the spatial degradation caused by the telescope diffraction, van Noort (2012) developed a new method, spatially coupled inversion, in which the spectropolarimetric data is degraded in a known way, using the telescope point spread function (PSF), and the atmospheric parameters over the whole field of view (FOV) of the data are simultaneously constrained.

In the spatially coupled inversion, Stokes profiles for all pixels in a given FOV are synthesized and then convolved with the PSF of the telescope, and then these are matched with the observed Stokes profiles until χ -squared is minimized; then physical parameters are inferred. This method allows accurate fitting of Stokes profiles over a large FOV, and improves signal-to-noise and spatial resolution of the inversion results. Further, the

spatially coupled inversion can be carried out at a higher pixel resolution than that of the observed magnetogram by artificially refining the pixel grid of the solution, thus, resolving additional substructures down to the diffraction limit of the telescope, that were not resolved with earlier, pixel based, inversions of Hinode (SOT/SP) data.

For exploring the internal structure of sunspot penumbra Tiwari et al. (2013) used this newly developed spatially coupled inversion code implemented in the SPINOR code (Frutiger et al. 2000), which returns depth-dependent physical parameters, based on their response functions to the used spectral lines. Tiwari et al. (2013, 2015) used a pixel size of $0.08''$ and the structures down to the diffraction limit of the telescope were resolved. A three-node inversion was performed and the best results obtained after several experiments were used for analysis. The physical parameters returned from the inversion are temperature T , magnetic field strength B , field inclination γ , field azimuth ϕ , line-of-sight velocity v_{LOS} , and a microturbulent velocity v_{mic} . Before the velocities were inferred, a velocity calibration was done by assuming that umbra, excluding UDs, is at rest. Maps of the sunspot in a few selected physical parameters from the inversion are shown in figure 2.

Selecting penumbral filaments: From the maps of the physical quantities returned from the inversions of the Hinode SOT-SP data of a sunspot, Tiwari et al. (2013) were able to isolate penumbral filaments. However, because a single parameter map was not sufficient to track full filaments, e.g., filament heads (the “head” of a filament is the part of the filament nearest to the sunspot umbra) were clearly visible in T and v_{LOS} maps but could not be detected in γ maps, and the tails (the “tail” of a penumbral filament is the part of the filament farthest from the sunspot umbra) of filaments could not be detected in T maps, Tiwari et al. (2013) combined T , v_{LOS} , and γ maps for selecting filaments. The selected penumbral filaments were de-stretched and straightened using bi-cubic spline interpolation and normalized to a certain length. To reduce fluctuations and to extract common properties to all filaments, they averaged filaments after sorting them into inner, middle, and outer filaments. Before the work of Tiwari et al. (2013), the full picture of a penumbral filament was not known (see, e.g., Borrero & Ichimoto 2011.)

Uniformity of properties in all penumbral filaments, and the “standard filament”: The selected penumbral filaments showed similar spatial properties everywhere, in the inner, middle, and outer parts of the sunspot penumbra. Therefore, Tiwari et al. (2013) averaged all selected penumbral filaments to create a “standard penumbral filament”. In figure 3, we display a few physical parameters of the standard filament at the optical depth unity. Please see Tiwari et al. (2013) for the plots of their depth-dependence and quantitative properties.

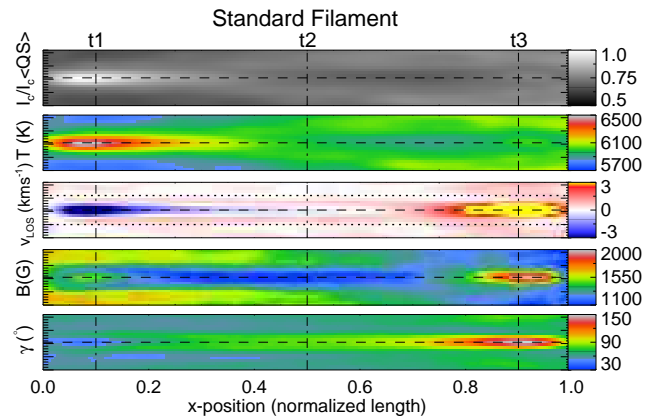


Fig. 3. Maps of five physical parameters of the standard penumbral filament, all at the surface of unit optical depth. Quantitative values along the longitudinal dashed line at the central axis of filaments and at three transverse cuts can be found in Tiwari et al. (2013). The total width including the surrounding mostly spine field is $1''.6$; the width of the filament itself, outlined for reference in the v_{LOS} map by two longitudinal dotted lines, is $0''.8$. [Reproduced from Tiwari et al. (2013) by permission of ESO.]

Size of filaments: The lengths of filaments varied from $2''$ to $9''$ with an average of $5'' \pm 1''.6$, whereas the width of each filament remained close to the averaged width of $0''.8$.

Thermal properties, heads of filaments — penumbral grains

All penumbral filaments contained a bright head in I_c and T (~ 6500 K) maps at the optical depth unity, with a rapid fall in temperature (and intensity) along their central axes towards the tail, the difference in the temperatures of the heads and the tails reaching up to 800 K. The teardrop-shaped heads of penumbral filaments were earlier referred to as penumbral grains (Muller 1973; Sobotka et al. 1999; Rimmele & Marino 2006; Zhang & Ichimoto 2013).

Dark lanes: A dark core along the central axis of the “standard filament” is clearly visible in the middle and higher photospheric layers (Tiwari et al. 2013); see Scharmer et al. (2002), Bellot Rubio et al. (2007), Langhans et al. (2007), and Rimmele (2008) for earlier reports of dark lanes in penumbral filaments. These can be as narrow as $0.1''$ (Schlichenmaier et al. 2016). The dark lanes are the locations of weak and more horizontal magnetic field than their surroundings, consistent with the observations of Bellot Rubio et al. (2007) and Langhans et al. (2007). The weak field at these locations results in a higher gas pressure thus raising the optical depth unity surface to the higher and cooler layers, which are then visible as dark lanes (Spruit & Scharmer 2006; Borrero 2007; Ruiz Cobo & Bellot Rubio 2008).

Magnetic field in penumbral filaments and convergence of surrounding spine field

With horizontal distance along a filament from its head, the field inclination changes from more

vertically up ($\gamma \sim 10\text{--}40^\circ$) in the head (where the field is strong), to horizontal in the middle (where the field is weaker), and then to downward ($\gamma \sim 140\text{--}170^\circ$) in the tail (where the field is stronger), thus making an inverse U shape. What happens to the field when it dips down into the photosphere at the tails of filaments is not known. They could form a sea-serpent, bipolar structure (Sainz Dalda & Bellot Rubio 2008; Schlichenmaier et al. 2010a), could remain below and disperse (Tiwari et al. 2013), or return back to the surface well outside the sunspot (Thomas et al. 2002).

The presence of more horizontal field in the middle of filaments at higher layers found by Tiwari et al. (2013) agrees with the inverse-U shape of penumbral filaments. The surrounding spine fields were found to diverge in the deepest layers and to converge together above the filament making a cusp shape, in agreement with the results of Borrero et al. (2008), who also analyzed Hinode data of a sunspot penumbra. The convergence of spine field with height over a filament agrees with the model of Solanki & Montavon (1993).

Absence of evidence of field-free gaps in penumbral filaments: Magnetic field strength is weaker along the middle of a filament but still has a value of ~ 1000 G (Tiwari et al. 2013). This indicates that the flow in filaments is not field-free, thus supporting the view that the Evershed flow is magnetized (Solanki et al. 1994; Borrero et al. 2005; Ichimoto et al. 2008a; Rempel 2012). In agreement with this result and with that of Borrero & Solanki (2008), recent deep-photospheric observations of sunspots in Fe I lines, at around 1565 nm found no evidence of the regions with weak ($B < 500$ G) magnetic fields in the sunspot penumbrae (Borrero et al. 2016).

Convective nature of penumbral filaments: All penumbral filaments display a clear pattern of convection both in the radial and azimuthal directions; upflows concentrate in the head (at ~ 5 km s $^{-1}$, on average) but continue along the central axis up to more than half of a filament. Strong downflows concentrate in the tail (at ~ 7 km s $^{-1}$, on average) of each filament. In addition weak but clear downflows (of 0.5 km s $^{-1}$) are visible along the side edges of penumbral filaments, see also Joshi et al. (2011); Scharmer et al. (2011); Scharmer & Henriques (2012); Ruiz Cobo & Asensio Ramos (2013); Scharmer et al. (2013), and Esteban Pozuelo et al. (2015). A scatter plot made by Tiwari et al. (2013) between T and v_{LOS} revealed that upflows are systematically hotter than downflows by some 800 K, thus quantitatively supporting convective nature of penumbral filaments.

Opposite polarity magnetic field at the sites of lateral downflows: In 20 of the 60 penumbral filaments studied by Tiwari et al. (2013) the narrow downflowing lanes at the sides of filaments

were found to carry opposite polarity magnetic field to that of spines and to that in the heads of filaments. Similar opposite polarity fields inside sunspot penumbrae were also reported by e.g., Ruiz Cobo & Asensio Ramos (2013), Scharmer et al. (2013), and Franz et al. (2016). The opposite magnetic polarity field along the filament sides was averaged out in the standard penumbral filament in figure 3.

The Evershed flow: Consistent with the presence of dominant upflows in the inner penumbrae and dominant downflows in the outer penumbrae (Franz & Schlichenmaier 2009; Tiwari et al. 2013, 2015, van Noort et al. 2013) the Evershed flow can be explained as a siphon flow in magnetized horizontal flux tubes (Meyer & Schmidt 1968; Solanki & Montavon 1993; Montesinos & Thomas 1997; Schlichenmaier et al. 1998; Ichimoto et al. 2007a; Jurčák et al. 2014). However, the siphon flow was ruled out in the recent past due to the presence of stronger magnetic field in the inner penumbrae than the outer penumbrae, which is instead more suitable to drive an inverse Evershed flow (inflow, due to higher gas pressure in the outer penumbrae and beyond), and also due to the support to the alternative idea of convection driving naturally the Evershed flow guided by inclined magnetic field (Hurlburt et al. 1996; Scharmer et al. 2008; Ichimoto 2010).

An enhanced magnetic field (1.5–2 kG, on average) was seen in the heads, and even stronger field (2–3.5 kG, on average) was found in the tails of penumbral filaments at $\log(\tau) = 0$ by Tiwari et al. (2013). This observation is consistent with a siphon flow to drive the Evershed flow, see also Siu-Tapia et al. (2017). However, because the geometrical heights of different parts of penumbral filaments are not known, no definite conclusion can yet be made. On the other hand the clear observation of both the radial and azimuthal convection supports the idea of Hurlburt et al. (1996) and Scharmer et al. (2008) that the presence of inclined field guides the convecting gas to generate an outflow, the Evershed flow. Moreover, the upflows being systematically hotter than the downflows in penumbral filaments support the idea that the gas rises hot near the head and along the central axis of a filament for more than half of its length, and is then carried outward along the horizontal magnetic field (as the Evershed flow) and across it in the azimuthal direction (Tiwari et al. 2013). The gas cools along the way before it sinks down at the side edges and in the tail of the filament. The Evershed flow does not stop abruptly at the outer boundary of sunspots but continues outside it in the moat region (Solanki et al. 1994; Rezaei et al. 2006; Shimizu et al. 2008a; Martínez Pillet et al. 2009).

Penumbral jets and bright dots: Penumbral jets are narrow transient bright events (10–20% brighter than the surrounding background), discovered by Katsukawa et al. (2007b) using the Ca II H-line filter on Hinode/SOT-FG. They have lifetimes of

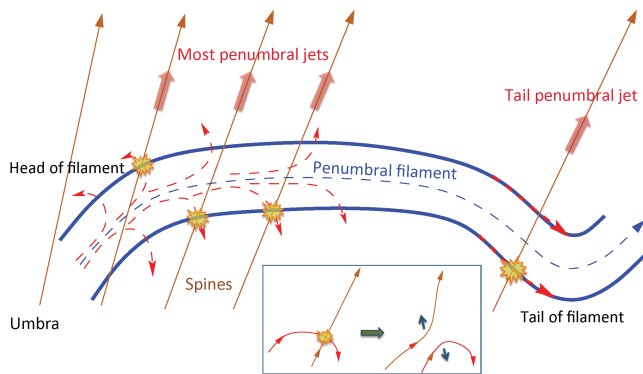


Fig. 4. A schematic sketch (not to scale) illustrating the formation of sunspot penumbral jets. All jets travel along the spine fields, which are more vertical in inner penumbrae (near filament heads). The red dashed lines with arrow heads show the direction of field lines in the filament. In a box in the middle bottom the magnetic configuration as well as the reconnection of spine field with opposite polarity field at the filament edge are shown. [Reproduced from Tiwari et al. (2016).]

less than a minute, widths of less than 600 km, lengths of multiple thousand km, and speeds of more than 100 km s^{-1} . These jets stream along the spine field, which get more inclined to the vertical with increasing horizontal radius in the penumbrae (Jurčák & Katsukawa 2008; Tiwari et al. 2015). Some of these jets heat the transition region directly above, but quantifying their coronal contribution requires further investigation (Tiwari et al. 2016).

Based on the new complete picture of penumbral filaments (Tiwari et al. 2013), Tiwari et al. (2016) proposed a modified view of formation of penumbral jets. The magnetic reconnection can take place between the spine field and the opposite polarity field in the sides of filaments, due to the obtuse angle between them, partly in agreement with the numerical modeling of Sakai & Smith (2008) and Magara (2010), rather than a component reconnection taking place between the spine fields of the same magnetic polarity and having an acute angle between them. A cartoon diagram of this possibility is shown in figure 4. Similar but more repetitive and larger jets at the tails of penumbral filaments were also detected by Tiwari et al. (2016) using Hinode/SOT-FG data.

Other dynamic events in sunspot penumbrae include moving bright dots, recently discovered by Tian et al. (2014) using IRIS data. Penumbral bright dots were also seen in Hi-C data (Alpert et al. 2016). Some of the bright dots and penumbral jets could be linked with each other and might have the same origin (Deng et al. 2016; Tiwari et al. 2016; Samanta et al. 2017); however, this subject requires extensive further investigation.

4 Long-lived controversies resolved

By exploring the complete picture of penumbral filaments using Hinode/SOT-SP data, and discovering that the physical proper-

ties of filaments change along their length, many of the long-standing controversies about structure of sunspot penumbrae are resolved. For example, the brightness and temperature of the downflowing regions can easily be confused with spines; both are darker regions than the heads of filaments. Lites et al. (1993) found more vertical fields/spines to be darker whereas Westendorp Plaza et al. (2001b) and Langhans et al. (2005) found the spines to be warmer. This could be because the heads of filaments were mistaken to be spines, both of these having similar field inclination. Similarly, by looking at different parts of filaments Borrero & Ichimoto (2011) concluded that the inter-spines are brighter filaments in the inner penumbrae and darker filaments in the outer penumbrae. The controversy also extends to whether the Evershed flow mainly takes place in the brighter or the darker regions of the penumbra (Lites et al. 1990; Title et al. 1993; Hirzberger & Kneer 2001; Westendorp Plaza et al. 2001a). However, from the fact that the upflows near heads are brighter and the downflows near tails are darker, one can interpret that the gas cools down as it travels along the filament central axis; thus the Evershed flow might be a natural outflow along the arched field. See Solanki (2003) for detailed literature on several such controversies and Tiwari et al. (2013) for their clarifications, thus highlighting the importance of resolving the complex magnetic, thermal, and flow structure of filaments for correctly interpreting observations of sunspot penumbrae.

5 Global properties of sunspots

Hinode data confirmed and clarified several global properties of sunspots found in the past and added new information; e.g., in the past magnetic field canopy was found by different authors to start at different locations in penumbrae (e.g., Borrero & Ichimoto 2011). It was verified by Tiwari et al. (2015) that the canopy starts only at the outer visible boundary of sunspots, in agreement with the results of Giovanelli (1980), Solanki et al. (1992, 1999), and Adams et al. (1993).

Penumbral spines and filaments: Spines have denser, stronger, and more vertical magnetic field in the inner penumbra. The spine field becomes less dense, less strong, but more inclined radially outward from the umbra. A comparison of scatter plots between B and γ for full sunspot and for only penumbral pixels revealed that spines have the same magnetic properties (except that these are more inclined) as the field in umbrae. Thus, Tiwari et al. (2015) concluded that spines are intrusions of umbral field into penumbrae. These locations of spines were consistently found to be locations of more force-free photospheric magnetic fields than elsewhere in sunspot penumbrae (Tiwari 2012).

Further, a qualitative similarity between scatter plots of dif-

ferent parameters for the standard penumbral filament (including its surrounding spines) and for sunspot penumbra led Tiwari et al. (2015) to conclude that sunspot penumbra is formed entirely of spines and filaments; no third component is present.

Peripheral strong downflows: Hinode observations showed the presence of systematic strong, often supersonic, downflows at the outer penumbral boundary of sunspots, with the presence of opposite polarity field therein to that of umbra and spines (e.g., Ichimoto et al. 2007a; Franz & Schlichenmaier 2009; Martínez Pillet et al. 2009; van Noort et al. 2013; Tiwari et al. 2015), but also see Jurčák & Katsukawa (2010) and Katsukawa & Jurčák (2010) for a different kind of flow reported in sunspot penumbrae. The strong peripheral downflows could be considered as the continuation of the Evershed flow outside sunspots (Solanki et al. 1994; Martínez Pillet et al. 2009).

van Noort et al. (2013) discovered the presence of the strongest magnetic fields and LOS velocities, ever reported in the photosphere, exceeding 7 kG and 20 km s⁻¹, respectively, in a few locations at the periphery of sunspots. They found a linear correlation between the downflow velocities and the field strength, which was in good agreement with MHD simulations. Possibly these peculiar downflows are induced by the accumulation and intensification of penumbral magnetic field by the Evershed flow. This is implied by the finding that these locations of strong downflows at the periphery of sunspots were the locations where tails of several penumbral filaments converge (Tiwari et al. 2013; van Noort et al. 2013).

Field gradients in sunspots: Generally, the field strength in sunspots decreases with increasing horizontal radius and height (Westendorp Plaza et al. 2001b; Mathew et al. 2003; Borrero & Ichimoto 2011; Tiwari et al. 2015). A decrease in the average field strength from 2800 G in umbra to 700 G at outer penumbral boundary in the deepest layers was found in a sunspot observed by Hinode (Tiwari et al. 2015). The sunspot umbra showed an average vertical field gradient of 1400 G km⁻¹ in the deepest layers, which drops rapidly with height, reaching to 0.95 G km⁻¹ at log(τ) = -2.5.

However, in addition to the canopy structure seen at the outer penumbral boundary, an inverse field gradient (field increasing with height) was found in the inner-middle penumbrae (Tiwari et al. 2015). Joshi et al. (2017) investigated this particular property of sunspots in details. They also found the presence of inverse gradient in MHD simulations. A closer look revealed the dominance of inverse gradients near the heads of penumbral filaments. The observed inverse field gradient could be a result of spine fields converging above filaments, the Stokes *V* signal cancellation at filament edges, or an artefact caused by highly corrugated optical depth unity surface in the inner penumbrae (Tiwari et al. 2015; Joshi et al. 2017). See a recent review on the

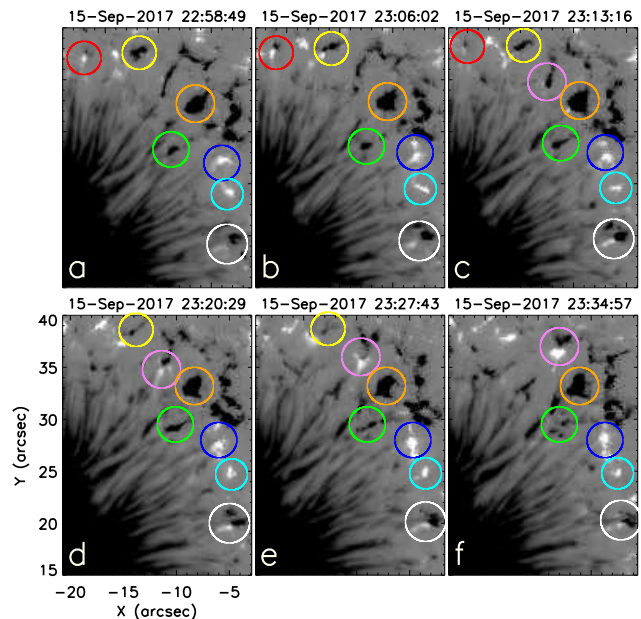


Fig. 5. Line-of-sight magnetic field maps of the upper right quarter of a sunspot penumbra, including its surrounding moat region, observed by SOT/SP in normal scan mode, thus having a pixel size of 0.16". Evolution of eight moving magnetic features are outlined by circles, each in a different color: red (panels a–c), yellow (panels a–e), orange (panels a–f), violet (panels c–f), green (panels a–f), blue (panels a–c), cyan (panels a–f), and ivory (panels a–f). The SP data used in this figure were inverted at the Community Spectropolarimetric Analysis Center (<http://www2.hao.ucar.edu/csac>).

height dependence of magnetic fields in sunspots by Balthasar (2018).

Moving magnetic features and sunspot decay: Moving magnetic features (MMFs, see figure 5) are small, unipolar or bipolar, structures of sizes $< 2''$ and lifetimes of 10 minutes to 10 hours. These move radially outward starting from the sunspot penumbra (or from within the moat region) with speeds of < 2 km s⁻¹ and eventually disappear in the network fields (Sheeley 1969; Harvey & Harvey 1973; Brickhouse & Labonte 1988; Hagenaar & Shine 2005; Ravindra 2006; Sainz Dalda & Bellot Rubio 2008; Lim et al. 2012; Li & Zhang 2013). Although MMFs are prominent sunspot features, they are also found in pores (Zuccarello et al. 2009; Criscuolo et al. 2012; Verma et al. 2012; Kaithakkal et al. 2017). Using Hinode SOT magnetograms Li & Zhang (2013) found that half of MMFs in a sunspot are produced within the penumbra and the other half originate within the moat region. They found that most of the MMFs formed in the moat are due to flux emergence. Once MMFs are formed, they start decaying by flux cancellation. The Evershed flow has been linked with the formation of MMFs (Martínez Pillet 2002; Zhang et al. 2007; Kubo et al. 2008a; Rempel 2015), but for disagreements, see Löhner-Böttcher & Schlichenmaier (2013).

MMFs are proposed to play a crucial role in the decay of sunspots (Harvey & Harvey 1973; Martínez Pillet 2002;

Hagenaar & Shine 2005). Consistent with the results of Hagenaar & Shine (2005), using Hinode SOT data Kubo et al. (2008b) and Kubo et al. (2008a) showed that in decaying sunspots the rate of the loss of magnetic flux ($8 \times 10^{15} \text{ Mx s}^{-1}$) in sunspots is very similar to the rate of the magnetic flux carried out by MMFs outwards, thus taking several weeks for a sunspot of 10^{22} Mx to completely decay. Kubo et al. (2008a) also showed that positive and negative polarities balance each other in the moat region, suggesting that most of the sunspot flux is transported to the moat region and then outward by MMFs, and then removed by flux cancellation in the network regions. The rate of flux transport by moat flows is consistent with that found in recent MHD simulations of Rempel & Cheung (2014) and Rempel (2015).

Sunspot formation: The formation of sunspots, being a subsurface process (Parker 1955), remains observationally more poorly understood than its decay. Sunspots form as a result of coalescence of small emerging magnetic elements (Zwaan 1985). Consistently, in the MHD simulations of Cheung et al. (2010); Stein & Nordlund (2012) and Rempel & Cheung (2014) flux emergence in the form of fragmented flux tubes (caused by subsurface convection) coalesce by horizontal inflow to make sunspots.

Much observational work has been devoted to penumbra formation. After a critical magnetic flux for umbra is reached any new flux joining the spot probably contributes to the formation of penumbra (Schlichenmaier et al. 2010b). Using Hinode data Shimizu et al. (2012) found that an annular feature in Ca II H in the form of a magnetic canopy surrounding the umbra in the chromosphere plays a role in the formation of penumbrae, thus proposing that the knowledge of chromospheric magnetic field is essential to understand the formation mechanism of sunspot penumbra. Kitai et al. (2014) concluded, again by using Hinode data, that penumbra can form in a few different ways, e.g., by active accumulation of magnetic flux, or by a rapid emergence of new magnetic flux, or by appearance of twisted or rotating magnetic tubes. The formation of sunspot penumbra is still not fully understood, and apparently depends on various factors, e.g., field strength, field inclination, size, amount of flux (Leka & Skumanich 1998; Rieutord et al. 2010; Rezaei et al. 2012; Kitai et al. 2014; Jurčák et al. 2015; Murabito et al. 2016; Jurčák et al. 2017; Murabito et al. 2017).

6 Summary and Future prospects

Sunspot physics has seen a major revolution in the first decade of the Hinode-era. Unprecedented observations of sunspots by the Hinode SOT have revealed or clarified several small-scale aspects of sunspots, especially umbral dots and light bridges in the umbra, filaments, spines and jets in the penumbra, field gra-

dient inversions in the inner penumbra, MMFs and peripheral downflows in the outer penumbra.

Hinode has solved several of the open questions that existed before the Hinode-era. Some of the most striking discoveries are umbral dots having dark lanes, and magnetoconvective flows in UD with the balanced mass-flux showing striking similarities with MHD models, granular light bridges having field free regions, internal structure of penumbral filaments, spines and filaments being the only components in the penumbra, MMFs being compatible with the idea of them being responsible for sunspot decay. The most striking new results are for the sunspot penumbra. Penumbral filaments are found to be elongated magnetized convective cells (Tiwari et al. 2013), qualitatively supporting recent magnetohydrodynamic (MHD) simulations (Rempel 2012). Several small-scale features were found to be part of penumbral filaments, e.g., penumbral grains are found to be the heads of filaments. Penumbral spines are observed to be true outward extension of umbral field. Sunspot penumbrae are formed entirely of spines and filaments (Tiwari et al. 2015).

Some enduring controversies about the complex penumbral structure, e.g., whether strands of more vertical field (spines) are warmer or cooler than strands of more horizontal field, whether the Evershed flow mainly takes place in dark or bright penumbral strands or there is no correlation between flow and brightness, whether more horizontal fields are found in darker or brighter penumbral regions, etc. (see for details Solanki 2003), have been resolved by uncovering the fact that spines and parts of filaments have some properties in common (Tiwari et al. 2013). A few of the unexpected discoveries about sunspots, using Hinode SOT data, include the magnetic field at the tails of penumbral filaments being stronger than that in the heads of penumbral filaments by 1–2 kG (Tiwari et al. 2013), the strongest magnetic field in many sunspots being found not in dark sunspot umbra, but rather often in light bridges (Okamoto & Sakurai 2018), or at the periphery of sunspots (van Noort et al. 2013).

Now we briefly mention some of the problems that should be addressed in future, i.e., by using future generation telescopes e.g., DKIST and SOLAR-C.

Concentrated downflows (with opposite polarity magnetic field in them to that of umbral field) surrounding umbral dots are expected from MHD simulations but have not been detected so far, probably because of insufficient spatial resolution of currently available magnetic field data. Absence of such concentrated downflows and opposite polarity field in higher resolution data would challenge present MHD simulations.

Because of the limited temporal cadence of spectropolarimetric data with Hinode, the lifetime of several small-scale features (e.g., penumbral filaments) remains poorly estimated. Further, how penumbral filaments form, evolve, and interact

with spines remains to be explored. Filaments and spines could result from loading/unloading of convecting gas onto/from the spine field. Or spines in penumbra could be a result of the over-turning convection taking place in-between them. Once the vertical magnetic field is sufficiently weak and the field is sufficiently inclined, a sub-surface convective instability within the sunspot can perhaps take place to form a penumbral filament. To address the above, we need to follow a sunspot penumbra of decent size in higher temporal and spatial resolution spectropolarimetric data for a couple of hours or more. Probably the formation mechanism of filaments and their interaction with spines also hold the answer to the formation mechanism of PJs and BDs, which may contribute to coronal heating above sunspots (Tiwari et al. 2016; Alpert et al. 2016, and references therein).

Multi-height spectropolarimetric data are needed to provide a 3-D picture of sunspots. A recent study by Joshi et al. (2016) showed the presence of fine-scale magnetic structure in the azimuthal direction in the upper chromospheric layers of sunspot penumbrae, consistent with that found in the photosphere, albeit with reduced amplitudes. Moreover, to understand the force balance in sunspots and their equilibrium (e.g., Venkatakrishnan & Tiwari 2010; Puschmann et al. 2010; Tiwari 2012), we need to develop a technique to estimate accurately the geometrical heights of different small-scale features in sunspots.

Acknowledgments

SKT would like to thank Dr. Ron Moore for helpful comments. Hinode is a Japanese mission developed and launched by ISAS/JAXA, with NAOJ as a domestic partner and NASA and STFC (UK) as international partners. It is operated by these agencies in cooperation with ESA and NSC (Norway). SKT's research was supported by an appointment to the NASA Postdoctoral Program at the NASA Marshall Space Flight Center, administered by Universities Space Research Association under contract with NASA. S.K.T. gratefully acknowledges his current support by NASA contracts NNG09FA40C (IRIS), and NNM07AA01C (Hinode).

References

- Adams, M., Solanki, S. K., Hagyard, M., & Moore, R. L. 1993, *Sol. Phys.*, 148, 201
- Alpert, S. E., Tiwari, S. K., Moore, R. L., Winebarger, A. R., & Savage, S. L. 2016, *ApJ*, 822, 35
- Asensio Ramos, A., Trujillo Bueno, J., & Landi Degl'Innocenti, E. 2008, *ApJ*, 683, 542
- Balthasar, H. 2018, *Sol. Phys.*, 293, 120
- Bellot Rubio, L. R., Schlichenmaier, R., & Langhans, K. 2010, *ApJ*, 725, 11
- Bellot Rubio, L. R., Tsuneta, S., Ichimoto, K., et al. 2007, *ApJL*, 668, L91
- Bharti, L. 2015, *MNRAS*, 452, L16
- Bharti, L., Joshi, C., & Jaaffrey, S. N. A. 2007, *ApJL*, 669, L57
- Bharti, L., Solanki, S. K., & Hirzberger, J. 2010, *ApJL*, 722, L194
- Borrero, J. M. 2007, *A&A*, 471, 967
- Borrero, J. M., & Ichimoto, K. 2011, *Living Reviews in Solar Physics*, 8, doi:10.12942/lrsp-2011-4
- Borrero, J. M., Lagg, A., Solanki, S. K., & Collados, M. 2005, *A&A*, 436, 333
- Borrero, J. M., Lites, B. W., & Solanki, S. K. 2008, *A&A*, 481, L13
- Borrero, J. M., & Solanki, S. K. 2008, *ApJ*, 687, 668
- Borrero, J. M., Asensio Ramos, A., Collados, M., et al. 2016, *A&A*, 596, A2
- Brickhouse, N. S., & Labonte, B. J. 1988, *Sol. Phys.*, 115, 43
- Cheung, M. C. M., Rempel, M., Title, A. M., & Schüssler, M. 2010, *ApJ*, 720, 233
- Cowling, T. G. 1953, *Solar Electrodynamics*, ed. G. P. Kuiper, 532
- Criscuolo, S., Del Moro, D., Giannattasio, F., et al. 2012, *A&A*, 546, A26
- Danilovic, S., Gandorfer, A., Lagg, A., et al. 2008, *A&A*, 484, L17
- Deng, N., Yurchyshyn, V., Tian, H., et al. 2016, *ApJ*, 829, 103
- Esteban Pozuelo, S., Bellot Rubio, L. R., & de la Cruz Rodríguez, J. 2015, *ApJ*, 803, 93
- Felipe, T., Collados, M., Khomenko, E., et al. 2016, *A&A*, 596, A59
- Feng, S., Zhao, Y., Yang, Y., et al. 2015, *Sol. Phys.*, 290, 1119
- Franz, M. 2011, PhD thesis, PhD Thesis, 2011, 176 pp.
- Franz, M., & Schlichenmaier, R. 2009, *A&A*, 508, 1453
- . 2013, *A&A*, 550, A97
- Franz, M., Collados, M., Bethge, C., et al. 2016, *A&A*, 596, A4
- Frutiger, C., Solanki, S. K., Fligge, M., & Bruls, J. H. M. J. 2000, *A&A*, 358, 1109
- Giovannelli, R. G. 1980, *Sol. Phys.*, 68, 49
- Gosain, S., Tiwari, S. K., & Venkatakrishnan, P. 2010, *ApJ*, 720, 1281
- Hagenaar, H. J., & Shine, R. A. 2005, *ApJ*, 635, 659
- Harvey, K., & Harvey, J. 1973, *Sol. Phys.*, 28, 61
- Heinemann, T., Nordlund, Å., Scharmer, G. B., & Spruit, H. C. 2007, *ApJ*, 669, 1390
- Hirzberger, J., Bonet, J. A., Sobotka, M., Vázquez, M., & Hanslmeier, A. 2002, *A&A*, 383, 275
- Hirzberger, J., & Kneer, F. 2001, *A&A*, 378, 1078
- Hurlburt, N. E., Matthews, P. C., & Proctor, M. R. E. 1996, *ApJ*, 457, 933
- Hurlburt, N. E., & Rucklidge, A. M. 2000, *MNRAS*, 314, 793
- Ichimoto, K. 2010, *Astrophysics and Space Science Proceedings*, 19, 186
- Ichimoto, K., Shine, R. A., Lites, B., et al. 2007a, *PASJ*, 59, S593
- Ichimoto, K., Suematsu, Y., Tsuneta, S., et al. 2007b, *Science*, 318, 1597
- Ichimoto, K., Tsuneta, S., Suematsu, Y., et al. 2008a, *A&A*, 481, L9
- Ichimoto, K., Lites, B., Elmore, D., et al. 2008b, *Sol. Phys.*, 249, 233
- Jahn, K., & Schmidt, H. U. 1994, *A&A*, 290, 295
- Joshi, J., Lagg, A., Hirzberger, J., Solanki, S. K., & Tiwari, S. K. 2017, *A&A*, 599, A35
- Joshi, J., Pietarila, A., Hirzberger, J., et al. 2011, *ApJL*, 734, L18
- Joshi, J., Lagg, A., Solanki, S. K., et al. 2016, *A&A*, 596, A8
- Jurčák, J., Bello González, N., Schlichenmaier, R., & Rezaei, R. 2015, *A&A*, 580, L1
- . 2017, *A&A*, 597, A60
- Jurčák, J., Bellot Rubio, L. R., & Sobotka, M. 2014, *A&A*, 564, A91
- Jurčák, J., & Katsukawa, Y. 2008, *A&A*, 488, L33
- . 2010, *A&A*, 524, A21
- Jurčák, J., Martínez Pillet, V., & Sobotka, M. 2006, *A&A*, 453, 1079
- Kaithakkal, A. J., Riethmüller, T. L., Solanki, S. K., et al. 2017, *ApJS*, 229, 13
- Katsukawa, Y., & Jurčák, J. 2010, *A&A*, 524, A20
- Katsukawa, Y., Yokoyama, T., Berger, T. E., et al. 2007a, *PASJ*, 59, S577
- Katsukawa, Y., Berger, T. E., Ichimoto, K., et al. 2007b, *Science*, 318,

1594

- Kitai, R., Watanabe, H., & Otsuji, K. 2014, PASJ, 66, S11
- Kitai, R., Watanabe, H., Nakamura, T., et al. 2007, PASJ, 59, S585
- Kosugi, T., Matsuzaki, K., Sakao, T., et al. 2007, Sol. Phys., 243, 3
- Kubo, M., Lites, B. W., Shimizu, T., & Ichimoto, K. 2008a, ApJ, 686, 1447
- Kubo, M., Lites, B. W., Ichimoto, K., et al. 2008b, ApJ, 681, 1677
- Lagg, A., Solanki, S. K., van Noort, M., & Danilovic, S. 2014, A&A, 568, A60
- Lagg, A., Woch, J., Krupp, N., & Solanki, S. K. 2004, A&A, 414, 1109
- Langhans, K., Scharmer, G. B., Kiselman, D., & Löfdahl, M. G. 2007, A&A, 464, 763
- Langhans, K., Scharmer, G. B., Kiselman, D., Löfdahl, M. G., & Berger, T. E. 2005, A&A, 436, 1087
- Leka, K. D., & Skumanich, A. 1998, ApJ, 507, 454
- Li, X., & Zhang, H. 2013, ApJ, 771, 22
- Lim, E.-K., Yurchyshyn, V., & Goode, P. 2012, ApJ, 753, 89
- Lites, B. W., Bida, T. A., Johannesson, A., & Scharmer, G. B. 1991, ApJ, 373, 683
- Lites, B. W., Elmore, D. F., Seagraves, P., & Skumanich, A. P. 1993, ApJ, 418, 928
- Lites, B. W., Skumanich, A., & Scharmer, G. B. 1990, ApJ, 355, 329
- Löhner-Böttcher, J., & Schlichenmaier, R. 2013, A&A, 551, A105
- Louis, R. E., Beck, C., & Ichimoto, K. 2014, A&A, 567, A96
- Louis, R. E., Bellot Rubio, L. R., Mathew, S. K., & Venkatakrishnan, P. 2009, ApJL, 704, L29
- Louis, R. E., Mathew, S. K., Bellot Rubio, L. R., et al. 2012, ApJ, 752, 109
- Magara, T. 2010, ApJL, 715, L40
- Martínez Pillet, V. 2002, Astronomische Nachrichten, 323, 342
- Martínez Pillet, V., Katsukawa, Y., Puschmann, K. G., & Ruiz Cobo, B. 2009, ApJL, 701, L79
- Mathew, S. K., Lagg, A., Solanki, S. K., et al. 2003, A&A, 410, 695
- Meyer, F., & Schmidt, H. U. 1968, Mitteilungen der Astronomischen Gesellschaft Hamburg, 25, 194
- Montesinos, B., & Thomas, J. H. 1997, Nature, 390, 485
- Moore, R., & Rabin, D. 1985, ARA&A, 23, 239
- Moore, R. L. 1981, Space Sci. Rev., 28, 387
- Muller, R. 1973, Sol. Phys., 29, 55
- Murabito, M., Romano, P., Guglielmino, S. L., & Zuccarello, F. 2017, ApJ, 834, 76
- Murabito, M., Romano, P., Guglielmino, S. L., Zuccarello, F., & Solanki, S. K. 2016, ApJ, 825, 75
- Okamoto, T. J., & Sakurai, T. 2018, ApJL, 852, L16
- Orozco Suárez, D., Bellot Rubio, L. R., Del Toro Iniesta, J. C., et al. 2007, PASJ, 59, S837
- Ortiz, A., Bellot Rubio, L. R., & Rouppe van der Voort, L. 2010, ApJ, 713, 1282
- Parker, E. N. 1955, ApJ, 121, 491
- Priest, E. 2014, Magnetohydrodynamics of the Sun
- Puschmann, K. G., Ruiz Cobo, B., & Martínez Pillet, V. 2010, ApJ, 720, 1417
- Ravindra, B. 2006, Sol. Phys., 237, 297
- Rempel, M. 2012, ApJ, 750, 62
- . 2015, ApJ, 814, 125
- Rempel, M., & Cheung, M. C. M. 2014, ApJ, 785, 90
- Rempel, M., & Schlichenmaier, R. 2011, Living Reviews in Solar Physics, 8, doi:10.12942/lrsp-2011-3
- Rempel, M., Schüssler, M., & Knölker, M. 2009, ApJ, 691, 640
- Rezaei, R., Bello González, N., & Schlichenmaier, R. 2012, A&A, 537, A19
- Rezaei, R., Schlichenmaier, R., Beck, C., & Bellot Rubio, L. R. 2006, A&A, 454, 975
- Riethmüller, T. L., Solanki, S. K., & Lagg, A. 2008, ApJL, 678, L157
- Riethmüller, T. L., Solanki, S. K., van Noort, M., & Tiwari, S. K. 2013, A&A, 554, A53
- Rieutord, M., Roudier, T., Rincon, F., et al. 2010, A&A, 512, A4
- Rimmele, T. 2008, ApJ, 672, 684
- Rimmele, T., & Marino, J. 2006, ApJ, 646, 593
- Rimmele, T. R. 1995, A&A, 298, 260
- . 1997, ApJ, 490, 458
- Rouppe van der Voort, L., Bellot Rubio, L. R., & Ortiz, A. 2010, ApJL, 718, L78
- Ruiz Cobo, B., & Asensio Ramos, A. 2013, A&A, 549, L4
- Ruiz Cobo, B., & Bellot Rubio, L. R. 2008, A&A, 488, 749
- Ruiz Cobo, B., & del Toro Iniesta, J. C. 1992, ApJ, 398, 375
- Sainz Dalda, A., & Bellot Rubio, L. R. 2008, A&A, 481, L21
- Sakai, J. I., & Smith, P. D. 2008, ApJL, 687, L127
- Samanta, T., Tian, H., Banerjee, D., & Schanche, N. 2017, ApJL, 835, L19
- Scharmer, G. B. 2009, Space Sci. Rev., 144, 229
- Scharmer, G. B., de la Cruz Rodríguez, J., Sütterlin, P., & Henriques, V. M. J. 2013, A&A, 553, A63
- Scharmer, G. B., Gudiksen, B. V., Kiselman, D., Löfdahl, M. G., & Rouppe van der Voort, L. H. M. 2002, Nature, 420, 151
- Scharmer, G. B., & Henriques, V. M. J. 2012, A&A, 540, A19
- Scharmer, G. B., Henriques, V. M. J., Kiselman, D., & de la Cruz Rodríguez, J. 2011, Science, 333, 316
- Scharmer, G. B., Nordlund, Å., & Heinemann, T. 2008, ApJL, 677, L149
- Scharmer, G. B., & Spruit, H. C. 2006, A&A, 460, 605
- Schlichenmaier, R., Bello González, N., Rezaei, R., & Waldmann, T. A. 2010a, Astronomische Nachrichten, 331, 563
- Schlichenmaier, R., Jahn, K., & Schmidt, H. U. 1998, ApJL, 493, L121
- Schlichenmaier, R., Rezaei, R., Bello González, N., & Waldmann, T. A. 2010b, A&A, 512, L1
- Schlichenmaier, R., von der Lühe, O., Hoch, S., et al. 2016, A&A, 596, A7
- Schlüter, A., & Temesváry, S. 1958, in IAU Symposium, Vol. 6, Electromagnetic Phenomena in Cosmical Physics, ed. B. Lehnert, 263
- Schmidt, H. U. 1991, Geophysical and Astrophysical Fluid Dynamics, 62, 249
- Schüssler, M., & Vögler, A. 2006, ApJL, 641, L73
- Sheeley, Jr., N. R. 1969, Sol. Phys., 9, 347
- Shimizu, T. 2011, ApJ, 738, 83
- Shimizu, T., Ichimoto, K., & Suematsu, Y. 2012, ApJL, 747, L18
- Shimizu, T., Lites, B. W., Katsukawa, Y., et al. 2008a, ApJ, 680, 1467
- Shimizu, T., Nagata, S., Tsuneta, S., et al. 2008b, Sol. Phys., 249, 221
- Shimizu, T., Katsukawa, Y., Kubo, M., et al. 2009, ApJL, 696, L66
- Siu-Tapia, A., Lagg, A., Solanki, S. K., van Noort, M., & Jurčák, J. 2017, A&A, 607, A36
- Skumanich, A., & Lites, B. W. 1987, ApJ, 322, 473
- Sobotka, M. 1997, in Astronomical Society of the Pacific Conference Series, Vol. 118, 1st Advances in Solar Physics Euroconference. Advances in Physics of Sunspots, ed. B. Schmieder, J. C. del Toro Iniesta, & M. Vázquez, 155

- Sobotka, M., Brandt, P. N., & Simon, G. W. 1999, *A&A*, 348, 621
- Sobotka, M., & Jurčák, J. 2009, *ApJ*, 694, 1080
- Sobotka, M., & Puschmann, K. G. 2009, *A&A*, 504, 575
- Socas-Navarro, H., Ruiz Cobo, B., & Trujillo Bueno, J. 1998, *ApJ*, 507, 470
- Solanki, S. K. 2003, *A&AR*, 11, 153
- Solanki, S. K., Finsterle, W., Rüedi, I., & Livingston, W. 1999, *A&A*, 347, L27
- Solanki, S. K., & Montavon, C. A. P. 1993, *A&A*, 275, 283
- Solanki, S. K., Montavon, C. A. P., & Livingston, W. 1994, *A&A*, 283, 221
- Solanki, S. K., Rüedi, I., & Livingston, W. 1992, *A&A*, 263, 339
- Spruit, H. C. 1977, *Sol. Phys.*, 55, 3
- . 1981, *Space Sci. Rev.*, 28, 435
- Spruit, H. C., & Scharmer, G. B. 2006, *A&A*, 447, 343
- Stein, R. F., & Nordlund, Å. 2012, *ApJL*, 753, L13
- Su, J. T., Sakurai, T., Suematsu, Y., Hagino, M., & Liu, Y. 2009, *ApJL*, 697, L103
- Suematsu, Y., Tsuneta, S., Ichimoto, K., et al. 2008, *Sol. Phys.*, 249, 197
- Thomas, J. H., & Weiss, N. O. 2004, *ARA&A*, 42, 517
- . 2008, *Sunspots and Starspots* (Cambridge University Press)
- Thomas, J. H., Weiss, N. O., Tobias, S. M., & Brummell, N. H. 2002, *Nature*, 420, 390
- Tian, H., Kleint, L., Peter, H., et al. 2014, *ApJL*, 790, L29
- Title, A. M., Frank, Z. A., Shine, R. A., et al. 1993, *ApJ*, 403, 780
- Tiwari, S. K. 2009, PhD thesis, Udaipur Solar Observatory/Physical Research Laboratory
- . 2012, *ApJ*, 744, 65
- Tiwari, S. K., Moore, R. L., Winebarger, A. R., & Alpert, S. E. 2016, *ApJ*, 816, 92
- Tiwari, S. K., van Noort, M., Lagg, A., & Solanki, S. K. 2013, *A&A*, 557, A25
- Tiwari, S. K., van Noort, M., Solanki, S. K., & Lagg, A. 2015, *A&A*, 583, A119
- Tiwari, S. K., Venkatakrishnan, P., Gosain, S., & Joshi, J. 2009a, *ApJ*, 700, 199
- Tiwari, S. K., Venkatakrishnan, P., & Sankarasubramanian, K. 2009b, *ApJL*, 702, L133
- Toriumi, S., Katsukawa, Y., & Cheung, M. C. M. 2015, *ApJ*, 811, 137
- Tritschler, A. 2009, in *Astronomical Society of the Pacific Conference Series*, Vol. 415, *The Second Hinode Science Meeting: Beyond Discovery-Toward Understanding*, ed. B. Lites, M. Cheung, T. Magara, J. Mariska, & K. Reeves, 339
- Tsuneta, S., Ichimoto, K., Katsukawa, Y., et al. 2008, *Sol. Phys.*, 249, 167
- van Noort, M. 2012, *A&A*, 548, A5
- van Noort, M., Lagg, A., Tiwari, S. K., & Solanki, S. K. 2013, *A&A*, 557, A24
- Venkatakrishnan, P., & Tiwari, S. K. 2009, *ApJL*, 706, L114
- . 2010, *A&A*, 516, L5
- Verma, M., Balthasar, H., Deng, N., et al. 2012, *A&A*, 538, A109
- Watanabe, H. 2014, *PASJ*, 66, S1
- Watanabe, H., Kitai, R., & Ichimoto, K. 2009, *ApJ*, 702, 1048
- Weiss, N. O. 2002, *Astronomische Nachrichten*, 323, 371
- Westendorp Plaza, C., del Toro Iniesta, J. C., Ruiz Cobo, B., & Martínez Pillet, V. 2001a, *ApJ*, 547, 1148
- Westendorp Plaza, C., del Toro Iniesta, J. C., Ruiz Cobo, B., et al. 2001b, *ApJ*, 547, 1130
- Yuan, D., & Walsh, R. W. 2016, *A&A*, 594, A101
- Zakharov, V., Hirzberger, J., Riethmüller, T. L., Solanki, S. K., & Kobel, P. 2008, *A&A*, 488, L17
- Zhang, J., Solanki, S. K., Woch, J., & Wang, J. 2007, *A&A*, 471, 1035
- Zhang, Y., & Ichimoto, K. 2013, *A&A*, 560, A77
- Zuccarello, F., Romano, P., Guglielmino, S. L., et al. 2009, *A&A*, 500, L5
- Zwaan, C. 1985, *Sol. Phys.*, 100, 397